NASA Technical Memorandum 107185
ASME–96–GT–482

Mixing of Multiple Jets With a Confined Subsonic Crossflow in a Cylindrical Duct

James D. Holdeman
Lewis Research Center
Cleveland, Ohio

David S. Liscinsky
United Technologies Research Center
East Hartford, Connecticut

Victor L. Oechsle
Allison Engine Company
Indianapolis, Indiana

G. Scott Samuelsen
University of California
Irvine, California

Clifford E. Smith
CFD Research Corporation
Huntsville, Alabama

Prepared for the
41st Gas Turbine and Aeroengine Congress
sponsored by the American Society of Mechanical Engineers
Birmingham, United Kingdom, June 10–13, 1996

National Aeronautics and
Space Administration

Mixing of Multiple Jets with a Confined Subsonic Crossflow in a Cylindrical Duct

James D. Holdeman
NASA Lewis Research Center
Cleveland, OH 44135

David S. Liscinsky
United Technologies Research Center
E. Hartford, CT 06108

G. Scott Samuelsen
University of California
Irvine, CA 92717

Victor L. Oechsle
Allison Engine Company
Indianapolis, IN 46206

Clifford E. Smith
CFD Research Corporation
Huntsville, AL 35805

Abstract

This paper summarizes NASA-supported experimental and computational results on the mixing of a row of jets with a confined subsonic crossflow in a cylindrical duct. The studies from which these results were derived investigated flow and geometric variations typical of the complex 3-D flowfield in the combustion chambers in gas turbine engines.

The principal observations were that the momentum-flux ratio and the number of orifices were significant variables. Jet penetration was critical, and jet penetration decreased as either the number of orifices increased or the momentum-flux ratio decreased. It also appeared that jet penetration remained similar with variations in orifice size, shape, spacing, and momentum-flux ratio when the number of orifices was proportional to the square-root of the momentum-flux ratio. In the cylindrical geometry, planar variances are very sensitive to events in the near-wall region, so planar averages must be considered in context with the distributions.

The mass-flow ratios and orifices investigated were often very large (mass-flow ratio >1 and ratio of orifice area-to-mainstream cross-sectional area up to 0.5), and the axial planes of interest were sometimes near the orifice trailing edge. Three-dimensional flow was a key part of efficient mixing and was observed for all configurations. The results shown also seem to indicate that non-reacting dimensionless scalar profiles can emulate the reacting flow equivalence ratio distribution reasonably well. The results cited suggest that further study may not necessarily lead to a universal "rule of thumb" for mixer design for lowest emissions, because optimization will likely require an assessment for a specific application.

Nomenclature

A_j/A_m	=	jet-to-mainstream area ratio
AC_d	=	$(A_j)(C_d)$
C	=	$(S/H)\sqrt{J}$
C_d	=	orifice discharge coefficient
D	=	diameter of cylindrical duct
d	=	orifice diameter
DR	=	jet-to-mainstream density ratio
H	=	duct height (rectangular)
J	=	jet-to-mainstream momentum-flux ratio
	=	$(DR)(V_j/U_m)^2$
	=	$(MR)^2/((DR)(C_d)^2(A_j/A_m)^2)$
L	=	long dimension of orifice
L/W	=	orifice aspect ratio
MR	=	jet-to mainstream mass-flow ratio
	=	w_j/w_m
n	=	number of holes around can
r	=	radial coordinate
R	=	can radius
S	=	lateral (circumferential) spacing between orifice centers
T	=	temperature
T_j	=	jet exit temperature
T_m	=	mainstream temperature
θ	=	$(T_m - T)/(T_m - T_j)$
U	=	axial velocity
U_m	=	mainstream velocity
V_j	=	jet velocity
w_j/w_m	=	$(\sqrt{DR})(\sqrt{J})(C_d)(A_j/A_m)$
	=	MR

w_j/w_T = jet-to-total mass flow ratio
= MR /(MR + 1)
W = short dimension of orifice
x = downstream coordinate
= 0 at leading edge of orifice
y = cross-stream (radial) coordinate
= 0 at wall
z = lateral (circumferential) coordinate
= 0 at centerplane

1. Introduction

Jets-in-crossflow have been extensively treated in the literature. Flows in which this is an integral constituent occur in a number of areas important in combustion and energy science and technology. In a gas turbine combustor for example, fuel and air mixing is important to combustor performance and emissions. Also, the mixing associated with arrays of jets in crossflow can play a critical role as in the dilution zone of a conventional combustor, and the mixing zone of a staged combustor such as the Rich-Burn/Quick-Mix/Lean-Burn (RQL) combustor. Although results reported to date have all contributed additional understanding of the general problem, the information obtained in them may not satisfy the specific needs of different applications.

One characteristic of jet-in-crossflow applications in gas turbine combustion chambers is that they are often confined mixing problems, with up to 80 percent of the total flow entering through the jets. The result is that the equilibrium mixing pattern and composition of the exiting flow may differ significantly from that of the entering mainstream flow.

A summary of NASA-supported research in the 1980's is given in Holdeman (1993). Several reports and papers have been published since the previous summary was presented that address cylindrical configurations. These include, Cline et al. (1995), Hatch et al. (1995a, 1995b), Holdeman et al. (1992), Holdeman (1993), Howe et al. (1991), Kroll et al. (1993), Leong et al. (1995), Liscinsky et al. (1993), Oechsle et al. (1992-1994), Oechsle & Holdeman (1995), Richards & Samuelsen (1992), Smith et al. (1991), Sowa et al. (1994), Talpallikar et al. (1992), Winowich et al. (1991), Yang et al. (1992), Zhu & Lai (1995).

2. Description of the Flowfield

Figure 1 shows a schematic of the flow in a cylindrical duct with injection from a row of jets at the wall. The scalar field results are often presented as plots of the temperature difference ratio, θ, where

$$\theta = \frac{(T_m - T)}{(T_m - T_j)}$$

or,

$$1-\theta = \frac{(T - T_j)}{(T_m - T_j)} \qquad (1)$$

Although T is used here, these parameters can be defined with concentrations or any conserved scalar. Also note that the jet fluid is identified by larger values of θ (i.e. θ = 1 if T = T_j, and θ = 0 if T = T_m). The equilibrium θ for any configuration is approximately equal to the fraction of the total flow entering through the jets, w_j/w_T. 1 - θ distributions have been used frequently in the RQL application, as temperature contour plots are often seen , and it seems more intuitive to think 1 = hot and 0 = cool. Note also that 1- θ is often referred to as mixture fraction in both the literature and this paper.

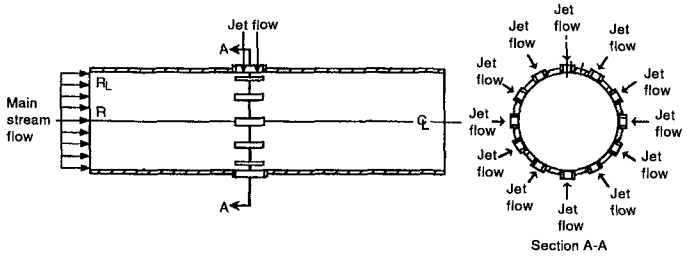

Figure 1: Schematic of typical configuration

Although it is recognized that a uniform temperature distribution may not always be desired, optimum is generally used herein (as in e.g. Holdeman, 1993) to identify flow and geometric conditions which lead to a uniform temperature distribution in a minimum downstream distance. What is perceived as "optimum" depends both on the application and the downstream distance. For example, if penetration is optimum, say at x/R = 1, the jets will probably overpenetrate farther downstream and underpenetrate upstream of this location.

The primary independent geometric variables are the spacing between adjacent orifices, S, the orifice diameter, d; the orifice aspect ratio, (L/W), and the orifice angle (with respect to the axial direction). Because the objective in combustor applications is to identify configurations to provide a desired mixing pattern within a given downstream distance, locations of interest are identified in intervals of the duct height (radius) rather than the orifice diameter, d. The primary independent flow variables are the jet-to-mainstream mass-flow ($MR = w_j/w_m$) and momentum-flux (J) ratios. These can be expressed as:

$$J = \frac{MR^2}{(DR)(C_d)^2(A_j/A_m)^2} \qquad (2)$$

It was reported in Holdeman (1993) that jet penetration and centerplane profiles were similar when the orifice spacing and the square root of the momentum-flux ratio were inversely proportional, i.e.:

$$C = (S/H)\sqrt{J} \qquad (3)$$

In a cylindrical duct, the radius, R, corresponds to the channel height, H in a rectangular duct. For single sided injection (such as for a can) the centerplane profiles are approximately centered across the duct height and approach an isothermal distribution in the minimum downstream distance when C = 2.5. This appeared to be independent of orifice diameter, as shown in both calculated and experimental profiles. The similarity of the profiles with the same orifice spacing but with different orifice diameters was also shown by Holdeman, Walker, & Kors (1973). Values of C in Eq. (3) which are a factor of 2 or more smaller or larger than the optimum correspond to underpenetration or overpenetration respectively.

For a can the optimum orifice spacing was specified at the radius which divides the can into equal areas. That is, the relationship of the spacing between jet centerlines to the number of holes around the circumference of the can would be

$$S = \frac{2\pi R_{1/2}}{n} \tag{4}$$

where,

$$R_{1/2} = \frac{H}{\sqrt{2}} \tag{5}$$

Substituting Eq. (5) into Eq. (4), and the resulting S/H into the spacing and momentum-flux relationship for a rectangular duct (Eq. (3)) gives the appropriate number of round holes as:

$$n = \frac{\pi\sqrt{2J}}{C} \tag{6}$$

It follows that the sector for each orifice would be 360/n degrees.

3. Results and Discussion

The following paragraphs describe the results from recent investigations in the context of the effects of the primary independent variables. Both experimental and computational studies were performed, but are interspersed here. The work cited was performed by Allison Engine Company, CFD Research Corporation, United Technologies Research Center, and the University of California, Irvine. Sources are identified when results are discussed, and specifics of the calculations or experiments, as appropriate, are given in the corresponding references.

All planar non-uniformity values are expressed as a variance from the mean values. Although the definitions used in the original papers differ slightly, they are essentially rms values. All orifices considered in this paper are thin (thickness/diameter < 0.25, and are plenum-fed with no bypass air.

Investigations published prior to 1991 were primarily in a rectangular duct, and at significantly lower mass-flow ratios than in more recent studies. A schematic showing the relative orifice size is given in Figure 2. Effects investigated included: 1) variation in momentum-flux ratio (J) at constant geometry; 2) variation of number of orifices at constant J; 3) comparison of slots & holes; 4) variation of slot aspect ratio; 5) variation of slanted slot angle; 6) results of orifice optimization; 7) effect of mixing duct size; 8) relation of mixing and emissions; and 9) effect of reaction. These are discussed in the following sections. Results from previous studies showed that the density ratio (DR) was not a significant variable at constant momentum-flux ratio (J).

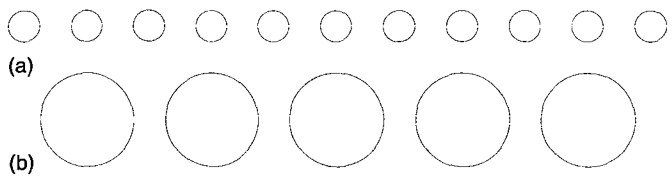

Figure 2: Example orifice geometry - (a) previous dilution jet mixing, (b) current investigations

3.1 Momentum-flux ratio

Based on previous studies which reported that the most important flow variable influencing the extent of jet mixing in a crossflow was the momentum-flux ratio, Hatch et al. (1995a) performed a series of tests with eight orifices at three representative J values. The results reaffirmed the importance of the momentum-flux ratio in determining the downstream flowfield.

A representative flowfield evolution for a baseline case of 8 round orifices at J near 25 (Hatch et al., 1995a), is shown in Figure 3. In the first plane (bottom), the absence of jet fluid is noted by the limited near zero mixture fraction values, while the presence of unmixed mainstream flow is apparent by the high mixture fraction values approaching 1 (unmixed jet fluid = 0 and unmixed mainstream fluid = 1). By the fifth plane downstream (up in Fig. 3), the jet and mainstream flow have mixed and have created a band of mixture fraction values that approach the equilibrium value. Mixture uniformity values calculated per plane provide the basis for the planar trend shown in Figure 4.

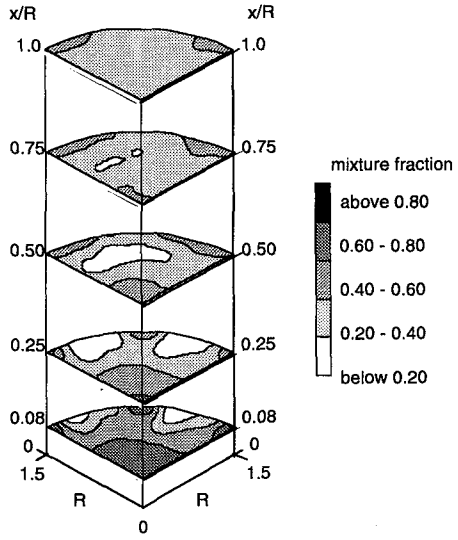

Figure 3: Mixture fraction, eight round hole configuration, J = 26.7 (data from Hatch et al. 1995a)

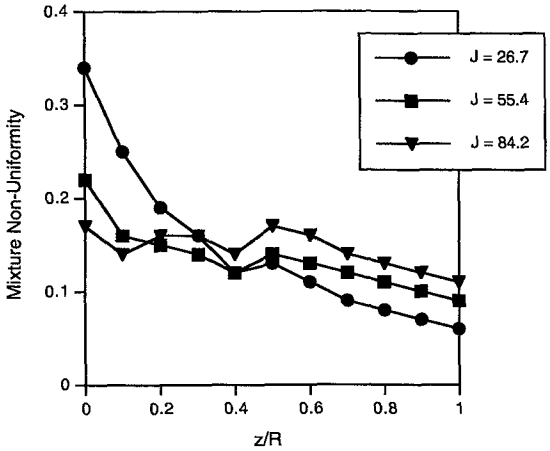

Figure 4: Mixture Non-Uniformity, Eight Round Hole Configuration (data from Hatch et al. 1995a)

A similar effect is apparent in the results of Talpallikar et al. (1991) as shown in Figure 5. The planar mixture non-uniformity for this case is shown in Figure 6 with a clearly defined optimum J for the configurations examined, with underpenetration to the left and overpenetration to the right.

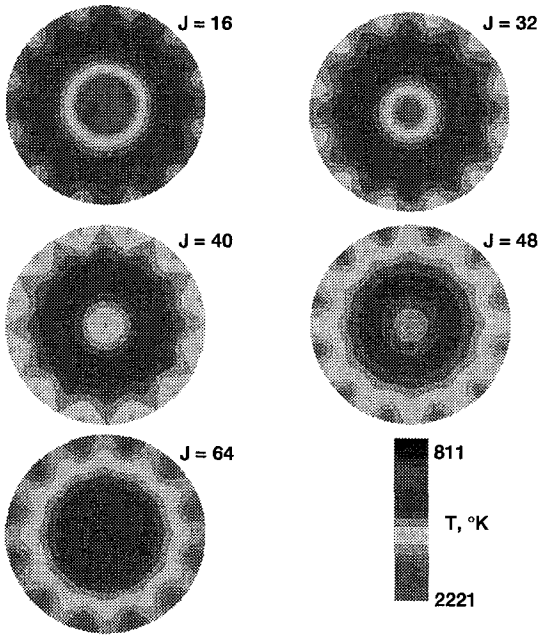

Figure 5: Temperature contour maps for reacting conditions: x/R=2.0 (data from Talpallikar et al. 1991)

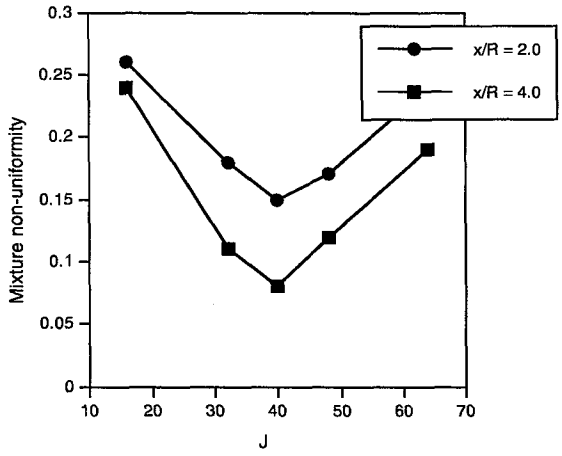

Figure 6: Mixture non-uniformity: reacting flow (data from Talpallikar et al. 1991)

The effect of momentum-flux ratio can also be seen in the experimental results of Vranos et al. (1991) as seen in Figure 7. A planar distribution from this study for slanted slots in shown in Figure 8. Differences in the J value of the minimum in these studies (for example Vranos, et al. (1991) and Talpallikar et al. (1991)) are due to slight differences in the conditions examined, and are unimportant.

The data shown in Figs. 7 and 8 are for slanted slots. The slant angle for slots is the angle between the long dimension and the axial direction. Note that slanted slots induce swirl although none is present in the main flow (Vranos et al. (1991)). It is also apparent in the results that although a local minimum is identified, it is possible to achieve low values of mixture non-uniformity at higher J values corresponding to overpenetration. This emphasizes that although planar averaged values are very useful and can provide insight, one cannot rely on them alone, and must also assess the flowfield distributions as shown in Figures 3, 5, & 7.

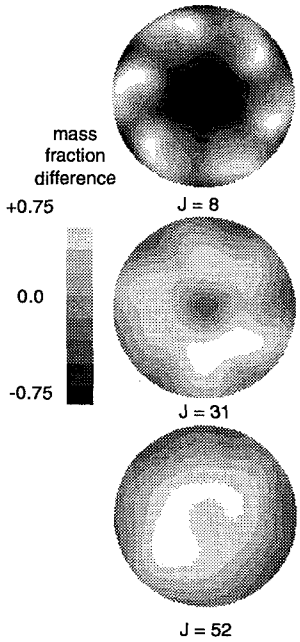

Figure 7: Effect of momentum-flux ratio on mixing from 6 slanted slots at x/R = 1.2 and DR = 1.0 (data from Vranos et al. 1991)

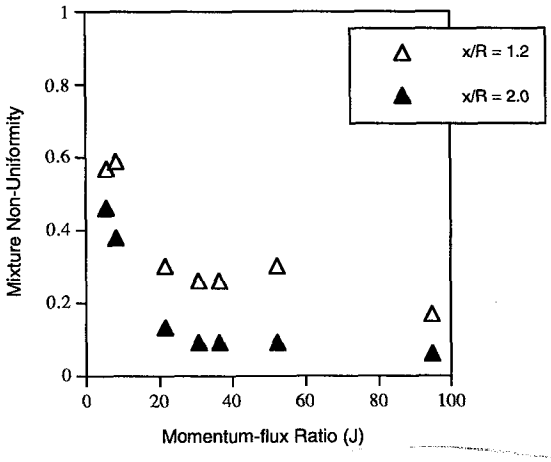

Figure 8: Mixture non-uniformity of slanted slots (data from Vranos et al. 1991)

3.2 Number of orifices

In general, the effect of increasing the number of orifices around the perimeter of a can is similar to the effect of decreasing the momentum-flux ratio (see Eq.(6)). Although this was also evident in previous results, the optimum was recently shown in the computational study by Smith et al. (1991). Since the optimum number relation, Eq. (6), was originally developed from computational results and round-hole data obtained in rectangular ducts at low mass-flow ratios, its applicability to other shapes and at higher mass-flow ratios was unknown.

Figure 9 shows isotherms of the centerplane (radial-axial plane through the geometric center of the orifice) for a different number of 4:1 aligned slots for J = 36. The jet penetration increases as an inverse function of the number of orifices. It is obvious that the flow from 14 slots is underpenetrated, whereas that for 10 is overpenetrated. Furthermore, the latter case can lead to upstream flow near the duct center, and can cause both poor mixing and high NO_x emissions (Talpallikar et al., 1990). For this configuration, 12 orifices seem to give optimum mixing whereas 11 would be predicted from Eq. (6).

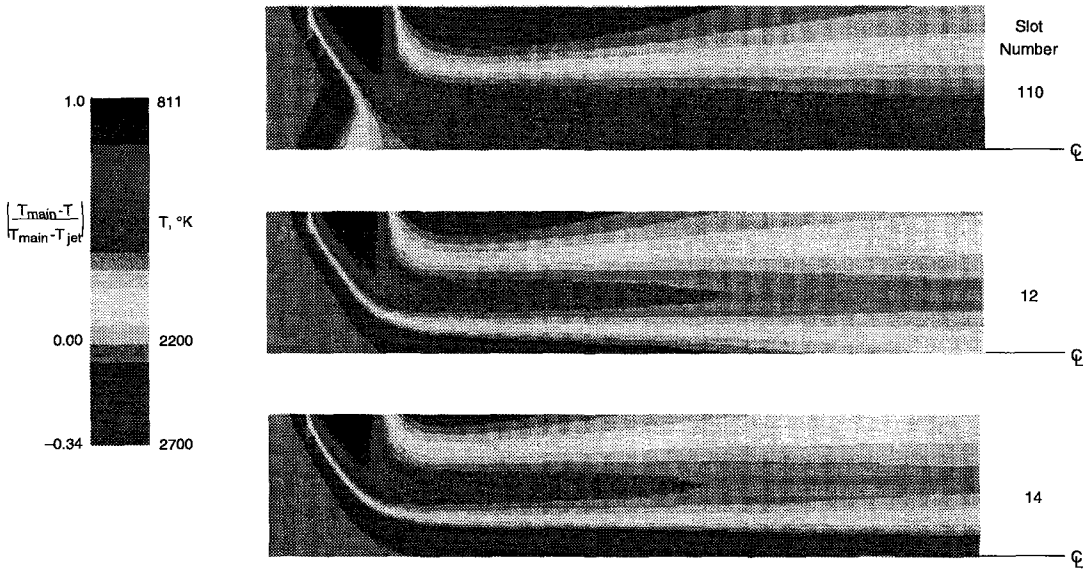

Figure 9: Predicted isothermal maps for J = 36; variation in number of slots (data from Smith et al. 1991)

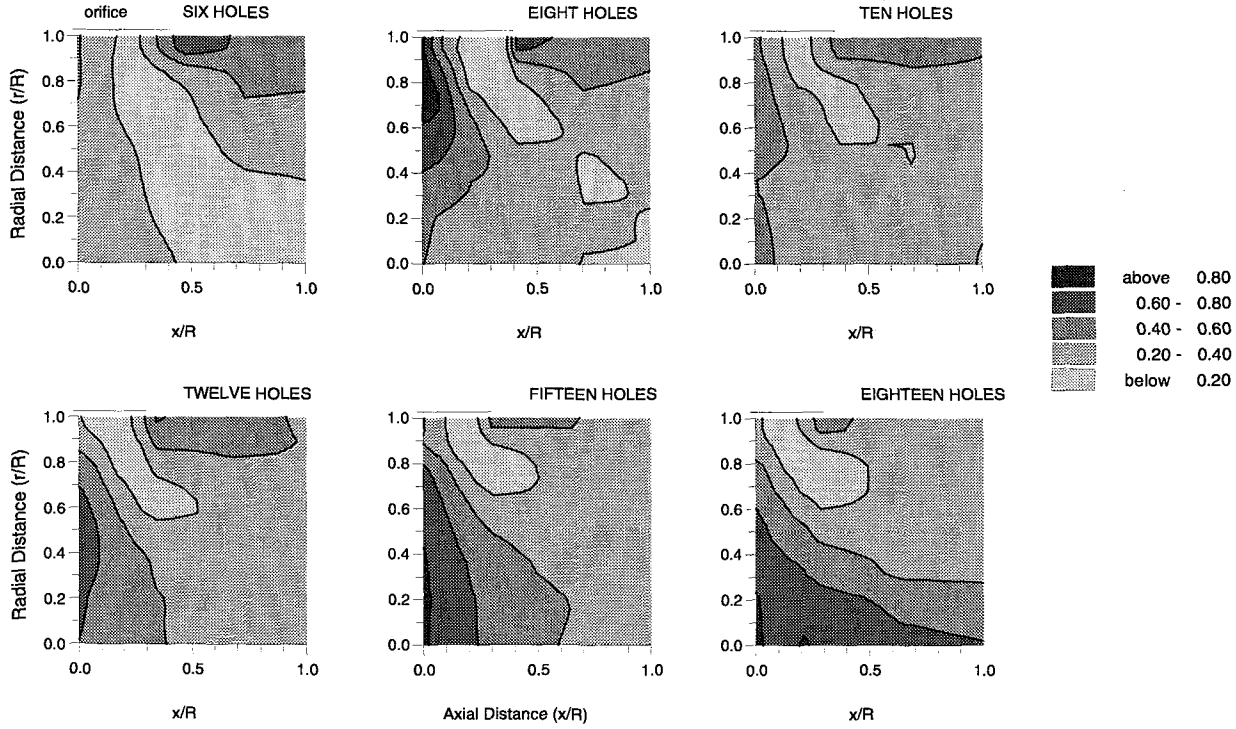

Figure 10: Local mixture fraction contours as the number of orifices are varied at J = 52. Radial distance ranges from the module centerline (r=0") to the wall (r=1.5"). Axial distance ranges from the orifice leading edge (z=0") to one duct radius downstream (z=1.5"). (data from Kroll et al. 1993)

The optimum number of round orifices was found experimentally for J = 52 to be between 12 and 15. This is shown in Figure 10 from Kroll et al. (1993). These distributions are radial-axial planes through the orifice center that were constructed from 100 thermocouple measurements in each of 5 planes. Here the jets enter from the can wall at the top, and proceed toward the can centerline at the bottom. The mainstream flow is from left to right. The mean jet trajectory can be traced by following the lowest values of mixture fraction downstream from the orifice.

3.3 Slots and holes

Representative still frames from movies of low speed flows from Vranos et al. (1991) are shown in Fig. 11. These indicate significant differences in the jet/jet and jet/mainstream interactions between slanted slots and round hole injectors. The jet exiting a round hole forms two counter rotating vortices of equal strength. The jet penetrates directly toward the center of the duct, and the jet cross section is stretched as J increases. The connecting sheet moves closer to the duct axis, but the vortices tend to remain near the wall.

The tendency of the vortices to stay near the wall is attributed, in part, to interaction between neighboring vortices, which act to translate adjacent vortices toward the duct wall. An additional influence of neighboring jets is to constrain the lateral spreading of the jet, and to spread it along its centerplane. This is particularly evident in the can as the lateral spread is increasingly restricted as the duct centerline is approached from the wall.

In contrast to the round jet, the slanted slot initially forms a pair of counter-rotating vortices which are of unequal size and strength. Larger vortices form downstream of the orifice leading edge and move toward the duct wall, while the smaller vortex moves away from the wall. There is considerable interaction between neighboring jets early in the injection process. In this case, unlike the round jet system, the induced velocity field is such that the vortex pair rotates about an axis connecting the vortex centers.

The bulk of the jet fluid identifies the location of the leading edge, thereby showing the direction that the slot is slanted (in Fig.7 the upstream edge of the slot is on the clockwise side). Furthermore, the slanted slot jet experiences a lateral force that causes it to rotate about the duct axis. The greatest circumferential velocity is due to the large vortex, and is near the wall. At the same time, the flow near the center is of the opposite sense so the net angular momentum is zero.

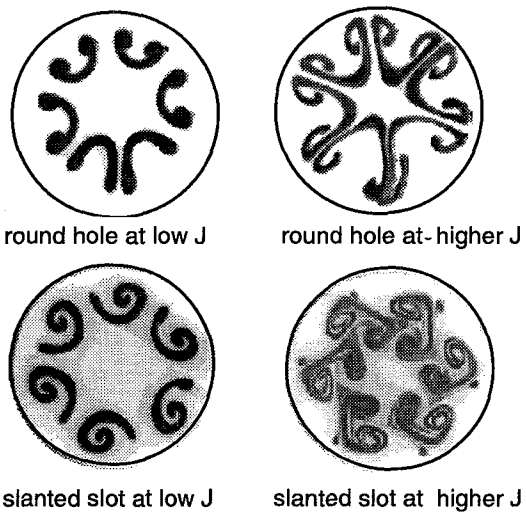

Figure 11: Frames from movies at low reynolds number (data from Vranos et al. 1991)

Planar non-uniformity for round holes and 45 degree slanted slots at x/R = 1.2 is shown in Figure 12. At this distance the two systems exhibit roughly the same average mixing, although the optimum J for round holes is less than that for slanted slots. It follows from the discussion in the previous section that the optimum spacing for slanted slots would be greater than for round holes for the same momentum-flux ratio.

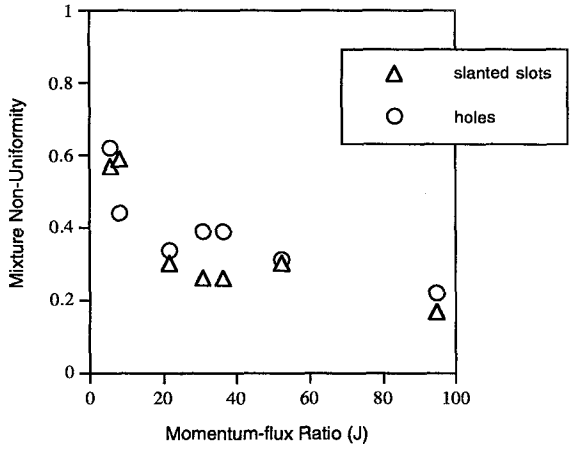

Figure 12: Mixture non-uniformity of equal area slanted slots and holes at x/R=1.2 (data from Vranos et al. 1991)

3.4 Slot aspect ratio

The slot aspect ratio affects 1) the amount of jet mass injected per unit length, and 2) the axial domain over which the mass is injected. Generally, increasing the aspect ratio (long:short dimension) of slanted slots decreases jet penetration. This is seen in Figure 13 from the computational results reported by Oechsle et al. (1992).

This effect can also be seen experimentally in the slanted slot results of Hatch et al. (1995a). For a given momentum-flux ratio and number of orifices, the smaller aspect ratio 45-degree slots penetrate farther into the crosstream. The larger aspect ratio slots, although penetrating less, create a stronger swirl component that enhances circumferential mixing. Figure 14 compares the mixture uniformity for 8:1 and 4:1 slanted slots. At the lowest and intermediate J values, the 4:1 geometry is a better mixer at all axial locations. At the highest J values tested, however, the 8:1 slot is competitive, and is the better mixer beyond x/R = 0.5. This is because of overpenetration of the jets at J = 84.2 for the 4:1 slots which improves mixing at the initial planes, but produces unmixed regions near the wall at downstream locations.

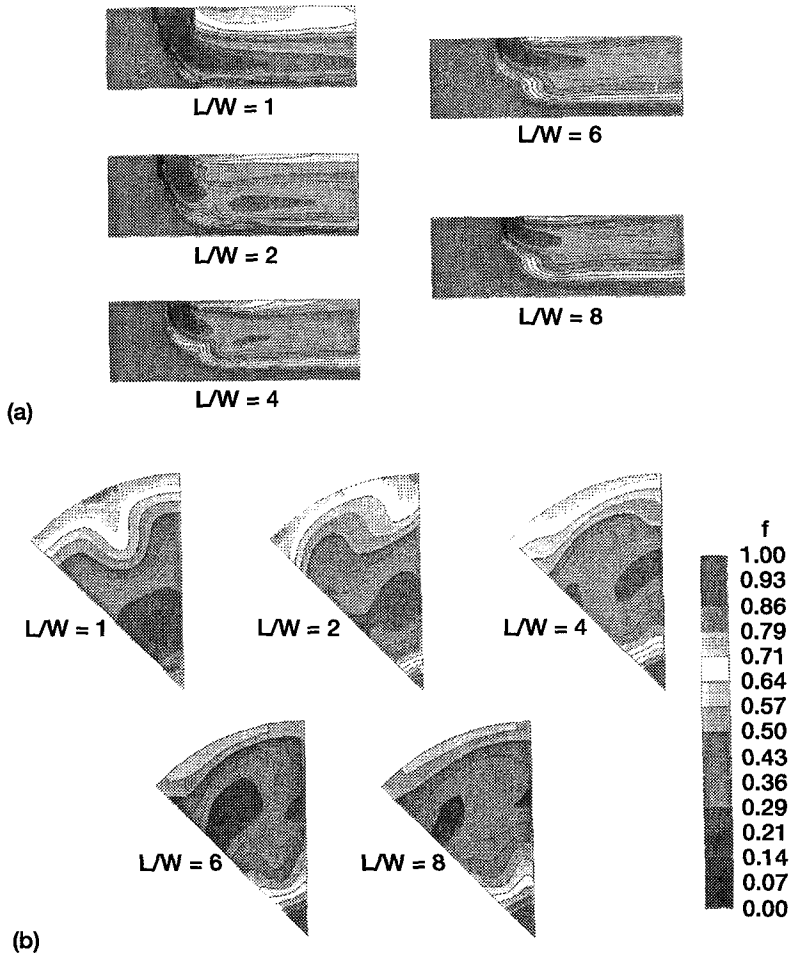

Figure 13: Effect of slot aspect ratio (L/W) on mixing for J = 20.5, (a) axial-radial plane through orifice center, (b) radial-tangential plane at x/R = 1. (data from Oechsle et al. 1992)

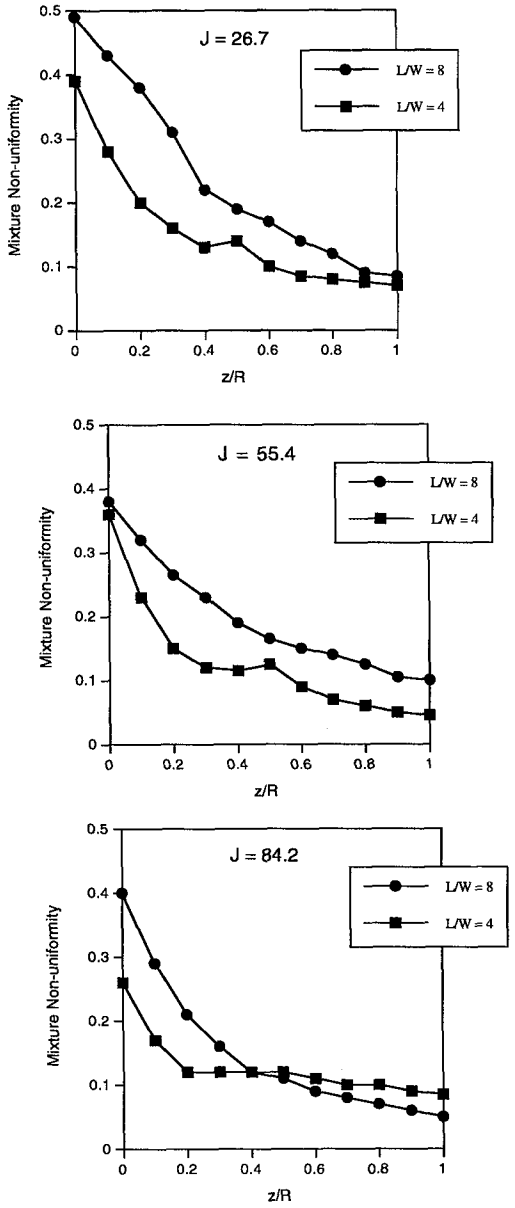

Figure 14: Effect of slot aspect ratio on mixture non-uniformity (data from Hatch et al. 1995a)

3.5 Slanted slot angle

The computational results in Figure 15 from Oechsle et al. (1992) indicate a significant decrease in jet penetration as slot slant angle is increased. Note that the slant angle is the angular deviation from the axial direction. This effect is also shown in the experimental results of Hatch et al. (1995a) that are shown in Figure 16.

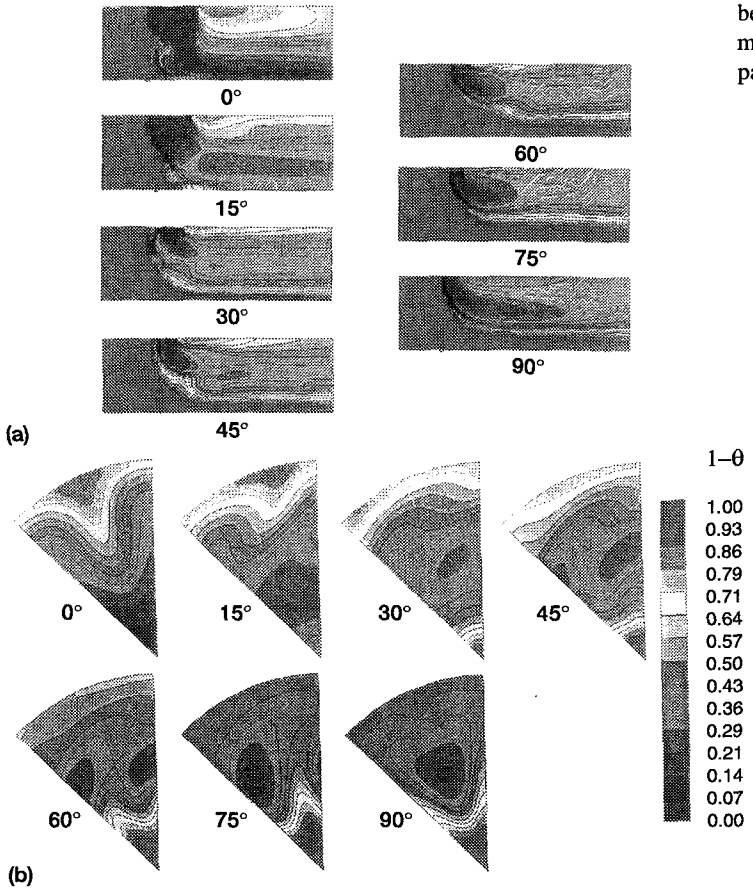

Figure 15: Effect of slot slant angle on mixing for J = 20.5,
(a) axial-radial plane through orifice center,
(b) radial-tangential plane at x/R = 1.
(data from Oechsle et al. 1992)

3.6 Orifice optimization

Sowa et al. (1994) engaged in a more comprehensive optimization scheme incorporating parameters such as the number of orifices, orifice aspect ratio, and orifice angle at a fixed momentum-flux ratio. Optimum mixing occurred when the mean trajectory lay between a radial distance of 50-65% from the mixer centerline at one duct radius downstream from the leading edge of the orifices. A numerical regression performed on the data yielded a non-linear relationship between the orifice configurations and the mixture uniformity. At the optimum number of orifices, both a round hole and a 5:1 22 degree slanted slot had minima in mixing uniformity. These distributions are shown on the next page in Figure 17.

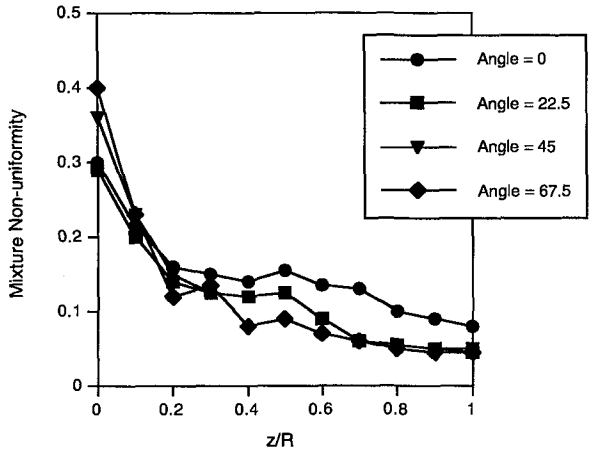

Figure 16: Effect of slot angle on mixture non-uniformity
(data from Hatch et al. 1995a)

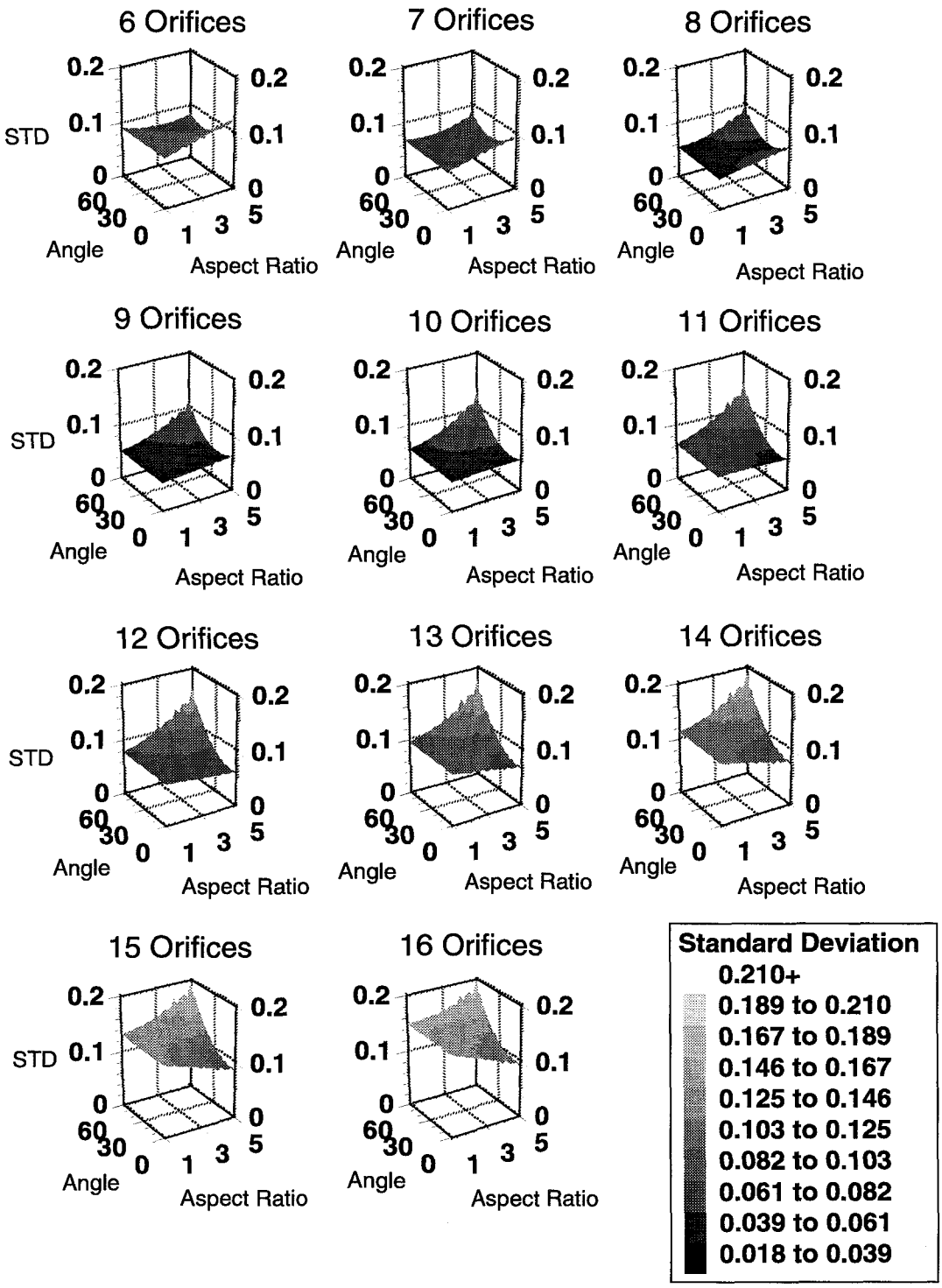

Figure 17: Predicted values of area weighted standard deviation "STD" for different orifice numbers as orifice aspect ratio and orifice angle are changed. (data from Sowa et al. 1994)

3.7 Mixing duct size

Three duct sizes were reported in Smith et al. (1991) using a previously optimized 12 slot geometry as a baseline case. The three mixing section diameters were 6, 5, & 4 inches (15.24, 12.70, & 10.16 cm). As the area was reduced, the velocity of the mainstream flow in the mixing section increased proportional to the area reduction. The resulting reduction in static pressure in the mixing section increases the pressure drop across the orifices, thus increasing the jet velocity. Both the jet and mainstream velocities increase, and these counterbalance such that the momentum-flux ratio remains constant as the mixing flow area is reduced.

The resultant mixing is shown in Figures 18 & 19 from Smith et al. (1991). The slot size was adjusted according to the variation in diameter of the mixing section to ensure a constant mass-flow ratio.

Figure 18 shows the temperature distributions in radial-axial planes through the orifice centerline for all three diameters. Figure 19 shows the corresponding distributions in a radial-transverse plane at one mixing section diameter downstream of the jet inlet. In this figure a full circle is shown, although the computations were performed for a 15 degree pie section. The similarity of the plots suggests that the flow was non-dimensionally identical for these cases.

However, the corresponding NO_x results (Smith et al., 1991) are not identical as shown in Figure 20. In this figure, NO_x production is plotted as a function of axial location for each of the three mixing section diameters. The NO_x Emission Index (EI (as defined by ARP 1256A)) at x/R = 2 for the 4" section is 70% less than that for the 6" section. For these cases, CO was completely depleted by x/R = 2.

The formation of NO_x is controlled by temperature, oxygen concentration, and residence time. Since mixing was identical, temperatures and oxygen concentrations must be identical, leaving only residence time to account for the difference. The NO_x reduction apparent in Fig. 20 is related to the decrease in residence time that occurs in smaller sections both through increased velocities and shorter mixing lengths. This is discussed in Smith et al. (1991).

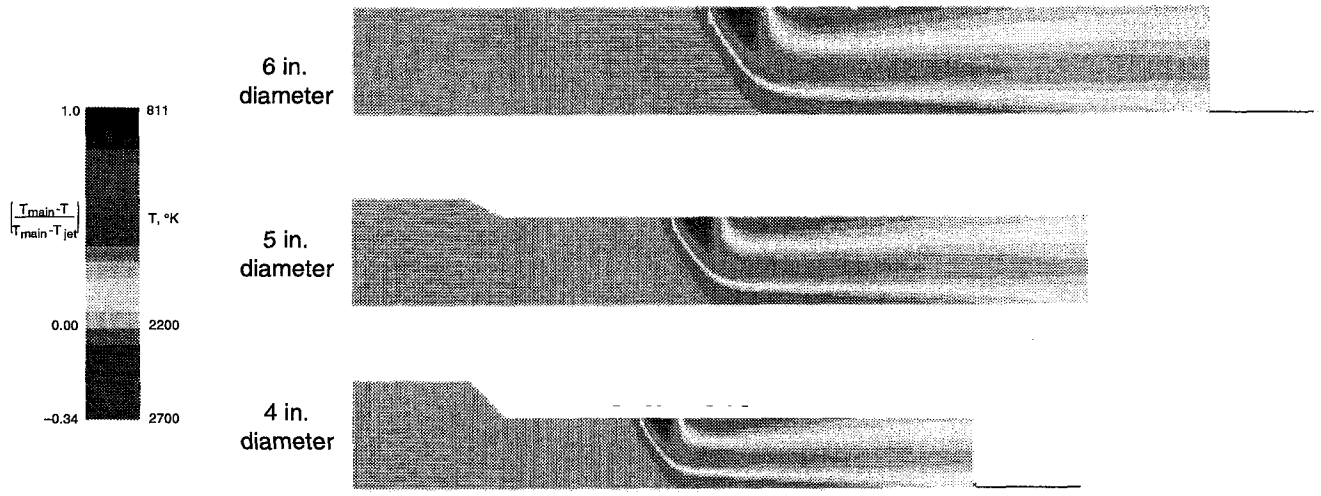

Figure 18: Predicted radial-axial plane isothermal maps (data from Smith et al. 1991) for J = 36; variation in mixing diameter.

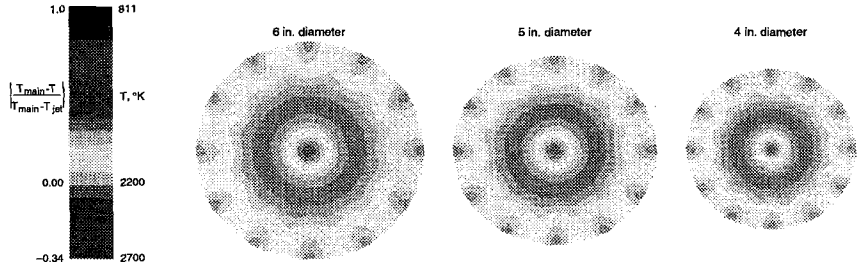

Figure 19: Predicted radial-tangential plane isothermal maps (x/R = 2.0) for J = 36; variation in mixing diameter. (data from Smith et al. 1991)

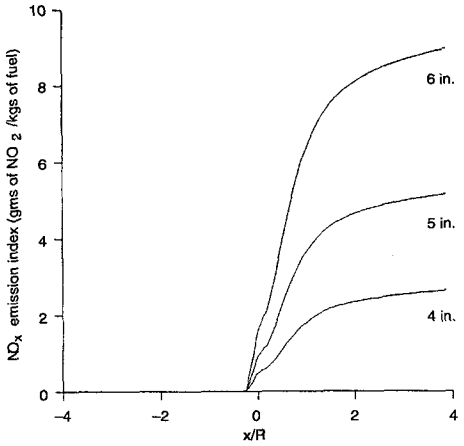

Figure 20: NO_x emission index for mixing diameters of 6", 5", and 4". (data from Smith et al. 1991)

3.8 Mixing and emissions

The relation between mixing and NO_x was investigated in Hatch et al. (1995b) using a procedure to infer NO_x signatures from non-reacting experimental data. The NO formation rate corresponding to the mixing flow field in Figure 3 is shown in Figure 21. The mixing and NO production field for the same configuration (8 round holes) at a higher momentum-flux ratio (J = 84.2) are shown in Figure 22. The Mixing Uniformity, NO Production Rate, and the Accumulated NO Produced for these configurations plus an intermediate J are shown in Figure 23.

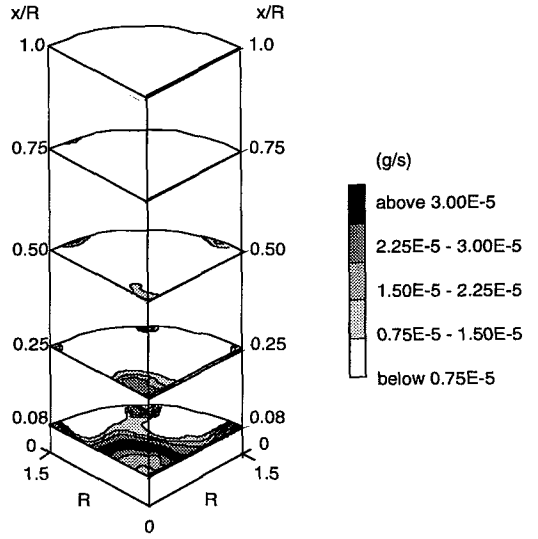

Figure 21: NO production, eight round hole configuration, J = 26.7 (data from Hatch et al. 1995b).

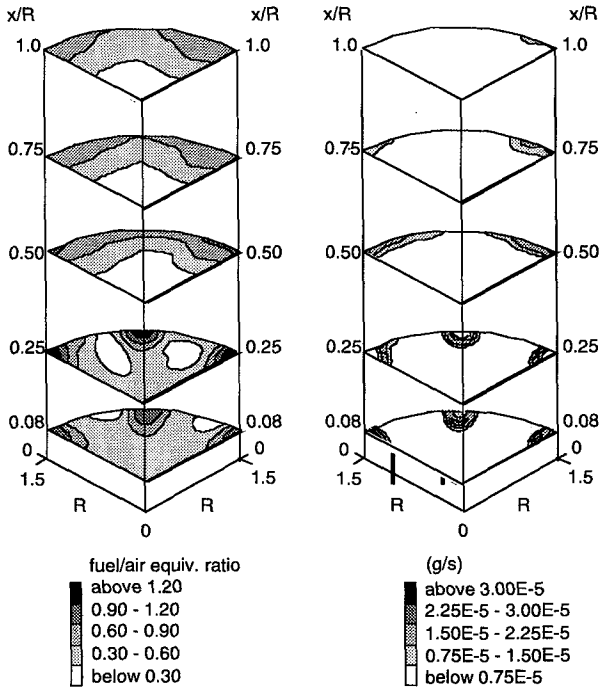

Figure 22: Equivalence ratio and NO production, eight round hole configuration, J = 84.2 (data from Hatch et al. 1995b).

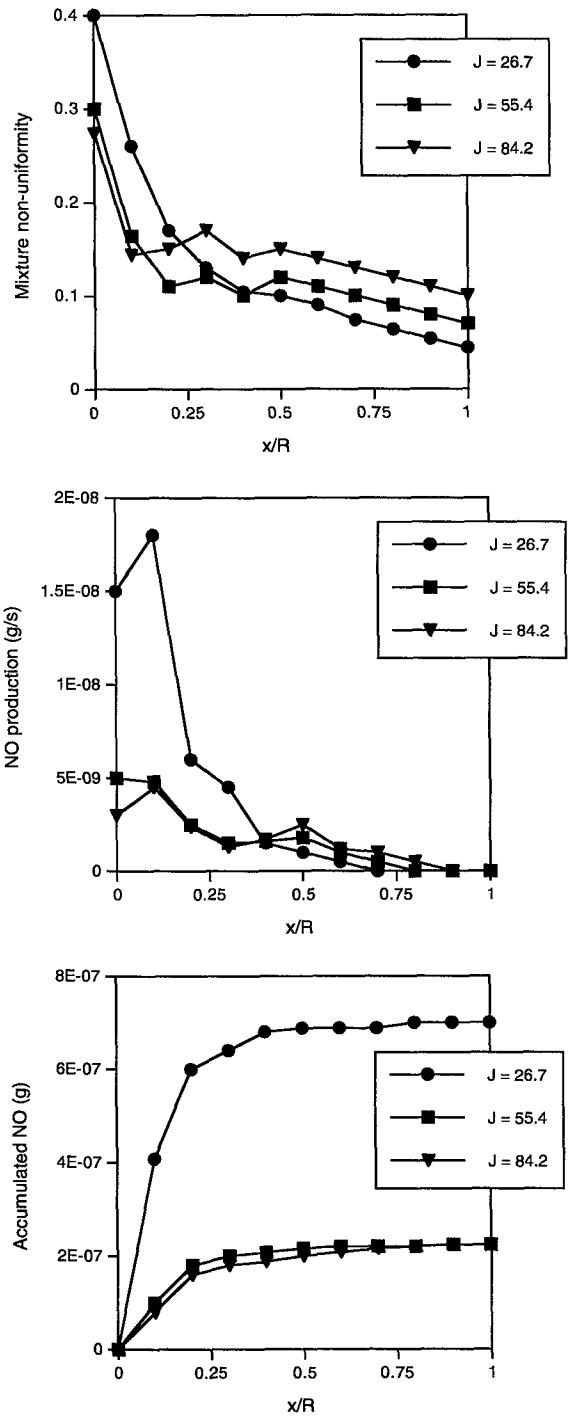

Figure 23: Planar results for eight round hole configuration (data from Hatch et al. 1995b).

The majority of nitric oxide is formed early in the injection. As a result the mixing processes in the initial region are critical in the overall emissions performance of the mixer. However, as can be seen in Figure 23, rapid early mixing due to overpenetrating jets (e.g. at J = 84.2 in Figures 22 & 23), does not necessary lead to a minimum production of NO.

For the range of momentum-flux ratios and orifice geometries examined in Hatch et al., (1995b) the round holes and 45 degree 4:1 slanted slots at J~55 yielded the best mixers from a NO perspective.

The relation between NO_x and mixing, for a fixed number of orifices, was also examined in the computations reported in Oechsle and Holdeman (1995). It was shown that, in general, statistical mixing parameters do not correlate with NO_x production rates at downstream axial locations (e.g. x/R = 1), as the planar variances lack historical information from throughout the mixing region.

NO_x production is shown to be highly related to the jet penetration. Overpenetrating configurations show increased NO_x production, as do underpenetrating cases. For example, at low J conditions, optimum penetration is achieved with round holes, and NO_x is minimum. At higher J's the jets overpenetrate and NO_x increases primarily due to its formation near the combustor walls. Similarly, jet penetration is optimum at higher momentum-flux ratios with large aspect ratios and slant angles, and NO_x is minimum for these configurations. At lower J's the jets severely underpenetrate, and NO_x increases due to its formation near the combustor centerline.

Although planar parameters don't seem to correlate with NO_x, one can infer relative NO_x production from the radial-axial and radial-transverse distributions, namely optimum penetration will generally yield minimum NO_x. One caveat is important here though: what one calls optimum depends on the axial location observed, that is, "optimum" penetration near the orifice will result in overpenetration farther downstream; and conversely "optimum" downstream penetration will look like underpenetration upstream of that location.

3.9 Reaction

The computational results reported by Oechsle et al. (1994) show that reacting flow distributions are very similar to non-reacting ones, provided that a conserved scalar is compared (which dimensionless temperature is not, as sources and sinks exist for this in reacting flows).

The dimensionless temperature distributions for the non-reacting cases are compared with normalized equivalence ratio distributions for the reacting flow cases. Radial-axial planes appear in Figure 24, while the corresponding radial-tangential planes at x/R = 1 are shown in Figure 25. These results suggest that the non-reacting temperature profiles can emulate the reacting flow equivalence ratio distribution reasonably well.

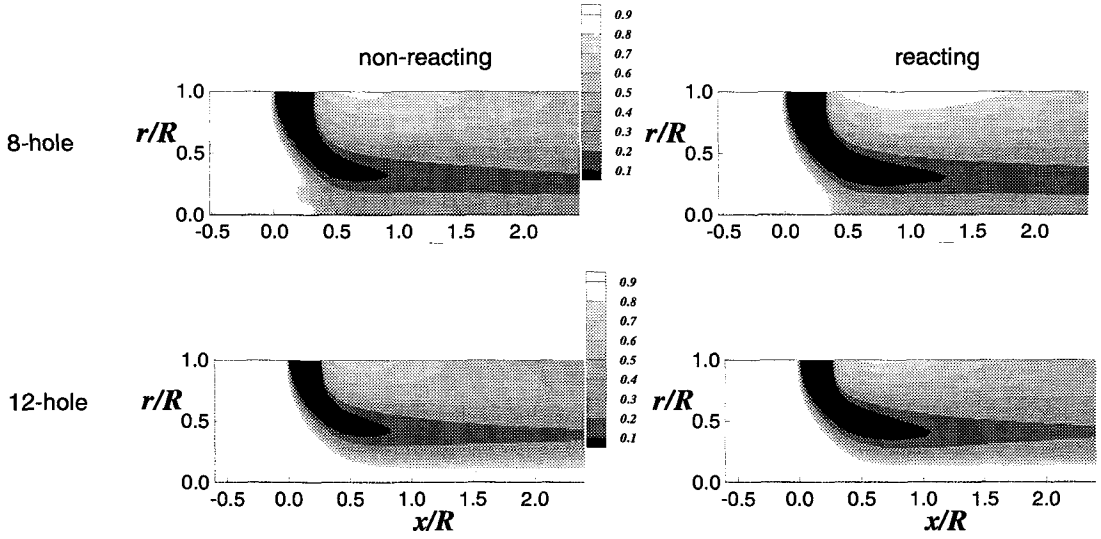

Figure 24: Normalized temperature distribution for non-reacting flow compared to the normalized equivalence ratio distribution for reacting flow (plane through the center of the jet) (data from Oechsle et al. 1994).

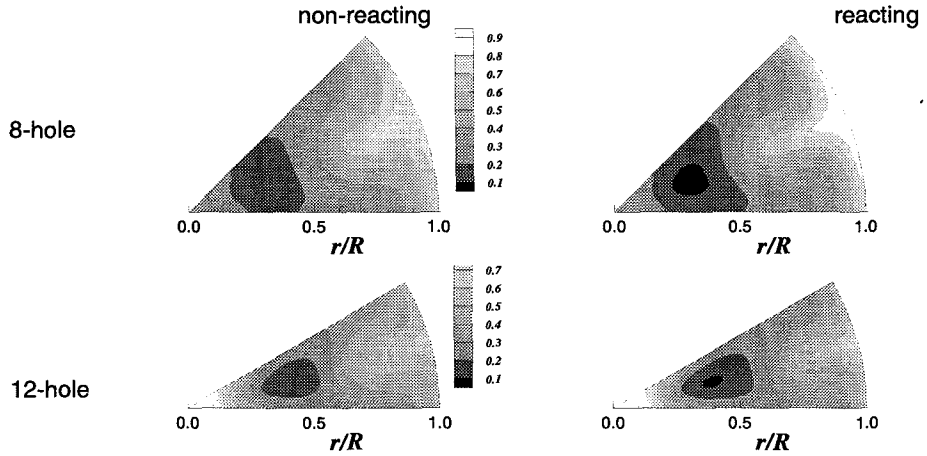

Figure 25: Normalized temperature distributionfor non-reacting flow compared to the normalized equivalence ratio distribution for the reacting flow for radial-tangential plane at x/R = 1 (data from Oechsle et al. 1994).

It is worth noting, however, that the non-reacting jets appear to interact more near the center of the mixer as compared to the corresponding reacting flow results. This is usually spotted by the upstream swirling flow production near where opposing jets merge. This was not observed in the 12-orifice cases investigated due to the much shallower penetration for these compared to the 8-orifice cases.

Reacting flow studies by Leong et al. (1995) were the first experimental characterization of jet mixing in a rich reacting cylindrical crossflow. Species concentration measurements were obtained for four round hole orifice configurations at a predetermined J. Jet penetration, as indicated by the maximum O_2 trajectory, was observed to affect reaction and mixing processes. Jet penetration toward the mid radius by x/R = 1 resulted in more lateral spreading of jet fluid which made available more fluid volume to react with the rich crossflow to produce CO_2. Figures 26 & 27 show that the 12-hole case produced an optimal jet (O_2) trajectory which gave a more evenly dispersed CO_2 distribution that most closely matches the concentration expected for the equilibrium equivalence ratio.

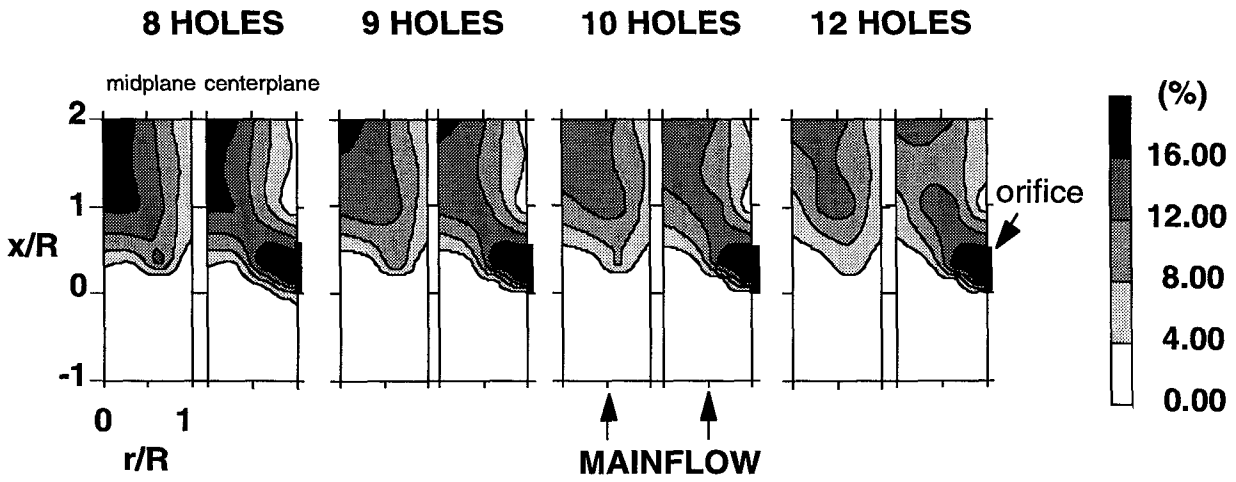

Figure 26: Averaged axial history of O_2 evolution at two radial-axial cross sections at J = 57 (data from Leong et al. 1995).

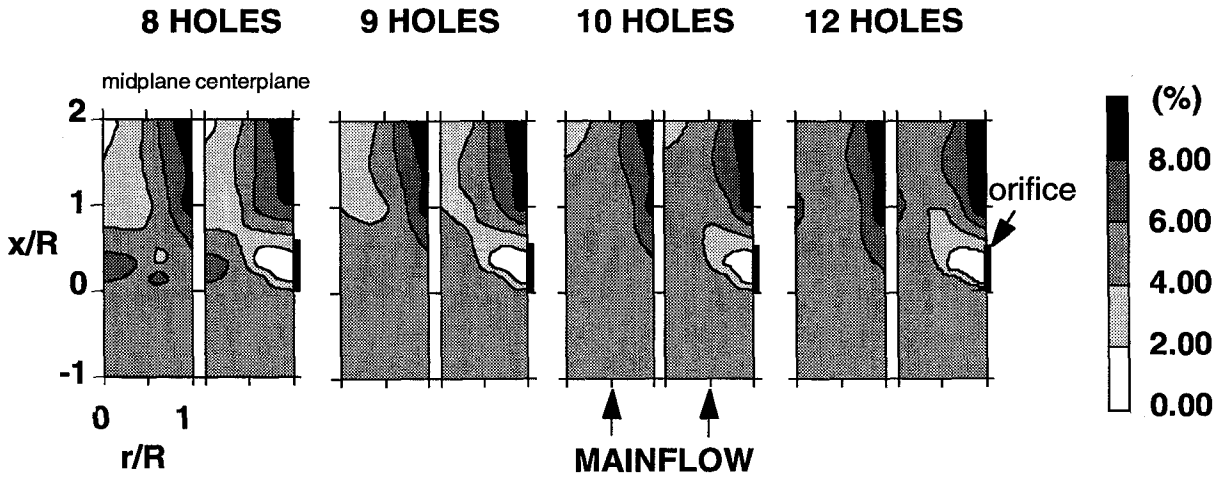

Figure 27: Averaged axial history of CO_2 evolution at two radial-axial cross sections at J = 57 (data from Leong et al. 1995).

4. Design Procedure

These results suggest that for a given momentum-flux ratio and downstream distance, combustor design procedure should first identify the circumferential orifice spacing required to obtain the desired penetration and profile shape. The orifice size would then be chosen to provide the required jet-to-mainstream mass-flow ratio. Some adjustments, including non-circular orifices or multiple rows, may be needed to arrive at the final design because the penetration varies slightly with orifice size and shape, and other parameters such as the combustor pressure loss; and the ratio of the orifice spacing to diameter must be monitored to insure that the suggested configuration is physically realistic.

Based on these results, the suggested procedure is, given mass-flow ratio, pressure drop, and channel height:

1) Choose desired orifice shape & C_d
2) Identify needed total orifice area
3) Calculate momentum-flux ratio (J)
5) Select number of orifices for optimum penetration
4) Calculate individual orifice size
6) Determine blockage, fit, etc.
7) Iterate to solution

Summary of Results

A) Several results from recent studies in a cylindrical duct are consistent with previous fresults from investigations in rectangular ducts. These include:

1) Variations in momentum-flux ratio and number of orifices have a significant effect on the flow distribution.

2) Optimum configurations may depend on given momentum-flux ratio, number of orifices, and orifice shape.
   a) Optimum spacing may vary with orifice shape.
   b) The optimum number of orifices (n) increases with increasing momentum-flux ratio (J). For most orifice shapes, n is proportional to $\sqrt{J}$.
   c) The same orifice shape may not be best for all momentum-flux ratios.
   d) What is perceived as "optimum" depends both on the application and the downstream distance.

3) Similar distributions can be obtained, independent of orifice size and shape, when n is proportional to $\sqrt{J}$. Although orifice configurations can be optimized for any J, a greater downstream distance is required for equilvalent mixing if either J and/or the optimum number of orifices is small.

4) The penetration of slanted slots is less than for aligned slots, or equal-area circular holes. Also, scalar distributions for slanted slots are rotated with respect to the injection centerplane.

5) For orifices that are symmetric with respect to the main flow direction, the effects of shape appear to be significant mostly in the region near the injection plane. Beyond e.g. x/R = 1, scalar distributions are expected to be similar to those observed from equally spaced equal-area circular orifices.

B) The minimization of NO production in a quick mixer will often require a tradeoff between effective initial mixing and effective mixing in the wall region downstream of the plane of injection.

C) The results cited suggest that further study may not necessarily lead to a universal "rule of thumb" for mixer design for lowest emissions, because optimization will likely require an assessment for a specific application.

D) The results shown seem to indicate that non-reacting dimensionless scalar profiles can emulate the reacting flow equivalence ratio distribution reasonably well.

Acknowledgments

The authors would like to acknowledge the contributions of the following: D.B. Bain, CFD Research Corporation (CFDRC); M.S. Hatch, Radian Corporation (formerly at the University of California, Irvine (UCI)); J.T. Kroll, UCI; M.Y. Leong, UCI; H.C. Mongia, GE Aircraft Engines (formerly with Allison Engine Company); B. True, United Technologies Research Center (UTRC); M.V. Talpallikar, CFDRC: W. Sowa, UTRC (formerly at UCI); and A. Vranos, University of Connecticut (formerly with UTRC).

References

ARP 1256A. Procedure for the Continuous Sampling and Measurement of Gaseous Emissions from Aircraft Turbine Engines. Society of Automotive Engineers, Inc., 1980.

Cline, M. C., Micklow, G. J., Yang, S. L., and Nguyen, H. L. (1995). Numerical Analysis of the Flowfield in a Staged Gas Turbine Combustor. Journal of Propulsion and Power, Vol. 11, No.5, Sep-Oct 1995, pp. 894-898.

Hatch, M.S., Sowa, W.A., Samuelsen, G.S. and Holdeman, J.D. (1995a). Jet Mixing into a Heated Cross Flow in a Cylindrical Duct: Influence of Geometry and Flow Variations. Journal of Propulsion and Power, Vol. 11, No. 3, May-Jun 1995, pp. 393-402 (see also AIAA-92-0773 & NASA TM 105390).

Hatch, M.S., Sowa, W.A., Samuelsen, G.S., and Holdeman, J.D. (1995b). Influence of Geometry and Flow Variation on NO Formation in the Quick Mixer of a Staged Combustor. To be published in Journal of Engineering for Gas Turbines and Power (see also NASA TM 105639).

Holdeman, J.D., Walker. R.E., and Kors, D.L. (1973). Mixing of Multiple Dilution Jets with a Hot Primary Airstream for Gas Turbine Applications. AIAA-73-1249 (also NASA TM-71426).

Holdeman, J.D. and Walker. R.E. (1977). Mixing of a Row of Jets With a Confined Crossflow. AIAA Journal, Vol. 15, No. 2, pp. 243ff (see also AIAA-76-48 (NASA TM-71821)).

Holdeman, J.D., Srinivasan, R., Reynolds, R., and White, C. (1992). Studies of the Effects of Curvature on Dilution Jet Mixing. Journal of Propulsion and Power, Vol. 8, No. 1, pp. 209-218 (see also AIAA-87-1953 (NASA TM 84878) & AIAA-88-3180 (NASA TM-100896)).

Holdeman, J.D. (1993). Mixing of Multiple Jets With a Subsonic Crossflow. Prog. Energy Combust. Sci., Vol.19, pp. 31-70 (see also AIAA-91-2458 & NASA TM 104412).

Howe, G.W., Li, Z., Shih, T.I.-P., and Nguyen, H.L. (1991). Simulation of Mixing in the Quench Zone of a Rich Burn-Quick Quench Mix-Lean Burn Combustor. AIAA Paper 91-0410.

Kroll, J.T., Sowa, W.A., Samuelsen, G.S., and Holdeman, J.D. (1993). Optimization of Circular Orifice Jets Mixing into a Heated Crossflow in a Cylindrical Duct. AIAA Paper 93-0249 (also NASA TM 105934).

Leong, M.Y., Samuelsen, G.S., and Holdeman, J.D. (1995). Jet Mixing in a Reacting Cylindrical Crossflow. AIAA Paper 95-3109 (also NASA TM 106975).

Liscinsky, D.S., Vranos, A., and Lohmann, R.P. (1993). Experimental Study of Cross-Stream Mixing in Cylindrical and Rectangular Ducts. NASA CR 187141.

Oechsle, V.L., Mongia, H.C., and Holdeman, J.D. (1992). A Parametric Numerical Study of Mixing in a Cylindrical Duct. AIAA Paper 92-3088, 1992 (also NASA TM 105695).

Oechsle, V.L., Mongia, H.C., and Holdeman, J.D. (1993). An Analytical Study of Jet Mixing in a Cylindrical Duct. AIAA Paper 93-2043 (also NASA TM 106181).

Oechsle, V.L., Mongia, H.C., and Holdeman, J.D. (1994). Comparison of the Mixing Calculations of Reacting and Non-reacting Flows in a Cylindrical Duct. AIAA Paper 94-0865 (also NASA TM 106435).

Oechsle, V.L. and Holdeman, J.D. (1995). Numerical Mixing Calculations of Confined Reacting Jet Flows in a Cylindrical Duct. AIAA Paper 95-0733 (also NASA TM 106736).

Richards, C.D. and Samuelsen, G.S. (1992). The Role of Primary Jets in the Dome Region Aerodynamics of a Model Can Combustor. Journal of Engineering for Gas Turbines and Power, Vol. 114, No. 1, pp. 20-26.

Sowa, W.A., Kroll, J.T., Samuelsen, G.S., and Holdeman, J.D. (1994). Optimization of Orifice Geometry for Crossflow Mixing in a Cylindrical Duct. AIAA Paper 94-0219 (also NASA TM 106436).

Smith, C.E., Talpallikar, M.V., and Holdeman, J.D. (1991). Jet Mixing in Reduced Flow Areas for Lower Emissions in Gas Turbine Combustors. AIAA Paper 91-2460 (also NASA TM 104411).

Talpallikar, Milind V., Smith, Clifford E., and Lai, Ming-Chia (1990) . Rapid Mix Concepts for Low Emission Combustors in Gas Turbine Engines. NASA CR 185292.

Talpallikar, M.V., Smith, C.E., Lai, M.-C., and Holdeman, J.D. (1992). CFD Analysis of Jet Mixing in Low NOx Flametube Combustors. Journal of Engineering for Gas Turbines and Power, April 1992, pp. 416-424 (see also ASME Paper 91-GT-217, NASA TM 104466).

Vranos, A., Liscinsky, D.S., True, B., and Holdeman, J. D. (1991). Experimental Study of Cross-Stream Mixing in a Cylindrical Duct. AIAA Paper 91-2459 (also NASA TM 105180).

Winowich, N.S., Moeykens, S.A., and Nguyen, H.L. (1991). Three-dimensional Calculations of the Mixing of Radial Jets from Slanted Slots with a Reactive Cylindrical Crossflow. AIAA Paper 91-2081.

Yang, S.L., Cline, M.C., Chen, H., and Chang, Y.-L. (1992). A Three-dimensional Grid Generation Scheme for Gas Turbine Combustors with Inclined Slots. ASME Computers in Engineering 1992, Vol. 2, pp. 43-51.

Zhu, G. and Lai, M.-C. (1995). A Parametric Study of Penetration and Mixing of Radial Jets in Necked-Down Cylindrical Cross-Flow. Journal of Propulsion and Power, Vol. 11, No. 2, Mar-Apr 1995, pp. 252-260 (see also AIAA-92-3091).

REPORT DOCUMENTATION PAGE

Form Approved
OMB No. 0704-0188

Public reporting burden for this collection of information is estimated to average 1 hour per response, including the time for reviewing instructions, searching existing data sources, gathering and maintaining the data needed, and completing and reviewing the collection of information. Send comments regarding this burden estimate or any other aspect of this collection of information, including suggestions for reducing this burden, to Washington Headquarters Services, Directorate for Information Operations and Reports, 1215 Jefferson Davis Highway, Suite 1204, Arlington, VA 22202-4302, and to the Office of Management and Budget, Paperwork Reduction Project (0704-0188), Washington, DC 20503.

1. AGENCY USE ONLY (*Leave blank*)	2. REPORT DATE	3. REPORT TYPE AND DATES COVERED
	April 1996	Technical Memorandum

4. TITLE AND SUBTITLE

Mixing of Multiple Jets With Confined Subsonic Crossflow in a Cylindrical Duct

5. FUNDING NUMBERS

WU–537–02–21–00

6. AUTHOR(S)

James D. Holdeman, David S. Liscinsky, Victor L. Oechsle, G. Scott Samuelsen, and Clifford E. Smith

7. PERFORMING ORGANIZATION NAME(S) AND ADDRESS(ES)

National Aeronautics and Space Administration
Lewis Research Center
Cleveland, Ohio 44135–3191

8. PERFORMING ORGANIZATION REPORT NUMBER

E–9996

9. SPONSORING/MONITORING AGENCY NAME(S) AND ADDRESS(ES)

National Aeronautics and Space Administration
Washington, DC 20546–0001

10. SPONSORING/MONITORING AGENCY REPORT NUMBER

NASA TM–107185
ASME–96–GT–482

11. SUPPLEMENTARY NOTES

Prepared for the 41st Gas Turbine and Aeroengine Congress sponsored by the American Society of Mechanical Engineers, Birmingham, United Kingdom, June 10–13, 1996. James D. Holdeman, NASA Lewis Research Center; David S. Liscinsky, United Technologies Research Center, East Hartford, Connecticut 06108; Victor L. Oechsle, Allison Engine Company, Indianapolis, Indiana 46206; G. Scott Samuelsen, University of California, Irvine, California 92717; and Clifford E. Smith, CFD Research Corporation, Huntsville, Alabama 35805. Responsible person, J.D. Holdeman, organization code 2650, (216) 433–5846.

12a. DISTRIBUTION/AVAILABILITY STATEMENT

Unclassified - Unlimited
Subject Category: 07

Available electronically at http://gltrs.grc.nasa.gov/GLTRS

This publication is available from the NASA Center for AeroSpace Information, (301) 621–0390.

12b. DISTRIBUTION CODE

13. ABSTRACT ***(Maximum 200 words)***

This paper summarizes NASA-supported experimental and computational results on the mixing of a row of jets with a confined subsonic crossflow in a cylindrical duct. The studies from which these results were derived investigated flow and geometric variations typical of the complex 3-D flowfield in the combustion chambers in gas turbine engines. The principal observations were that the momentum-flux ratio and the number of orifices were significant variables. Jet penetration was critical, and jet penetration decreased as either the number of orifices increased or the momentum-flux ratio decreased. It also appeared that jet penetration remained similar with variations in orifice size, shape, spacing, and momentum-flux ratio when the number of orifices was proportional to the square-root of the momentum-flux ratio. In the cylindrical geometry, planar variances are very sensitive to events in the near-wall region, so planar averages must be considered in context with the distributions. The mass-flow ratios and orifices investigated were often very large (mass-flow ratio >1 and ratio of orifice area-to-mainstream cross-sectional area up to 0.5), and the axial planes of interest were sometimes near the orifice trailing edge. Three-dimensional flow was a key part of efficient mixing and was observed for all configurations. The results shown also seem to indicate that non-reacting dimensionless scalar profiles can emulate the reacting flow equivalence ratio distribution reasonably well. The results cited suggest that further study may not necessarily lead to a universal "rule of thumb" for mixer design for lowest emissions, because optimization will likely require an assessment for a specific application.

14. SUBJECT TERMS

Dilution; Cylindrical; Jet mixing; Gas turbine; Emissions; Combustion chamber

15. NUMBER OF PAGES

17

16. PRICE CODE

A03

17. SECURITY CLASSIFICATION OF REPORT	18. SECURITY CLASSIFICATION OF THIS PAGE	19. SECURITY CLASSIFICATION OF ABSTRACT	20. LIMITATION OF ABSTRACT
Unclassified	Unclassified	Unclassified	